International Journal of Automation Mechatronics & Robotics – IJAMR
Volume 1 : Issue 1 *[ISSN 2374 – 1546]*
Publication Date : 09 January 2014

Design and Implementation of an Image-Based Controller for an Inverted Pendulum

Ying-Shing Shiao, Keng-Hao Chang, Ching-Wei Wu, Yun-Hao Tsai

***Abstract*—The conventional inverted pendulum was equipped with potentiometers to measured pendulum angles and cart positions. This paper use a CCD camera combined with image processing to measure feedback signal of rod angles and cart positions. The state space equations of an inverted pendulum and the image processing algorithms are used to design an image-based inverted pendulum controller. Controller parameters are obtained by using the linear quadratic regulator design and by the calibrations of image processing algorithms. The experimental results verify the proposed image servo controller can control an inverted pendulum in stable.**

***Keywords*—Inverted Pendulum, Images Servo Controller, Linear Quadratic Regulator(LQR).**

I. Introduction

Inverted pendulum system is an unstable system and is easily influenced by noises, so an inverted pendulum system is suitable for testing the performances of control theory. Traditionally, rod angles and cart positions of an inverted pendulum are measured by potentiometers. In this paper a camera with image processing algorithms are used to measure the rod angles and cart positions to get more flexible motion control and to get good performances in disturbances.

There are many inverted pendulum system such as rotational modes, cart-type double or triple link, and parallel double shown in the references [1], [2], [3], and [4]. Controller designs of these systems have their own difficulty. S. Nundrakwang et al [5] presented a hybrid controller which combine PD controller and state feedback controller. After the system start-up, the PD controller is used first to control the sagging pendulum to upright position, and then switch to the state feedback controller to make the inverted pendulum stability. H. Hirata et al. [6] proposed the two kinds of self-tuning control scheme to control a rotary inverted pendulum.

This self-tuning controller has two-stage. The adaptive control method of the variable structure system is used in the first stage to control the angle of pendulum rotation. While the pendulum is swing to the angle to close zero, it is switched to the second phase in which the LQ (Linear Quadratic) controller gets the rotary inverted pendulum in stability. In 1998, M. E. Magana and F. Holzapfel [7] used the CCD camera to grab images via image processing to calculate the inverted pendulum rod angles which are transmitted by using the RS-232 to the fuzzy logic controller that is a formation of visual feedback controls the inverted pendulum system. This experimental system includes the mechanical components (pulley, pendulum, and DC motor), visual unit (CCD camera and image grab card), and fuzzy controller. Longer processing time is the disadvantage of image processing to measure pendulum angles and cart positions with non-contact. Due to image processing, the discriminant errors of cart positions and rod angles make the vision control is not easy. The experimental result is the inverted pendulum with 2.7° offset in a 400ms oscillation period. Although the performance of visual feedback is not better than the conventional method, the visual feedback of the control problem is worth to be explored. The advantage and shortcoming of fuzzy controller and PID controller used in the inverted pendulum control are compared by B. Kosko [8], L. Wang [9], T. Brem [10], and M. I. H. Nour et al. [11]. The self-adaptive fuzzy control can overcome the uncertainly problem in nonlinear system. Fuzzy control relies on good rules of thumb to achieve the control objectives. The conventional PID controller used to control the high-order and multi-variable system is less performances.

This paper proposes the treatments for image processing with less time to get the measurement features of rod and cart for realizing the visual servo control of an inverted pendulum, which is organized as the follows. In section II the structure of an inverted pendulum cart is described and the inverted pendulum motion is formulated. The proposed image processing algorithms used for rod and cart segmentation as well as the implementation of visual controller which combining the image processing results and the LQR are illustrated in section III. The experimental results are shown in section IV. The conclusions and recommendations are discussed in section V.

II. Inverted Pendulum Model

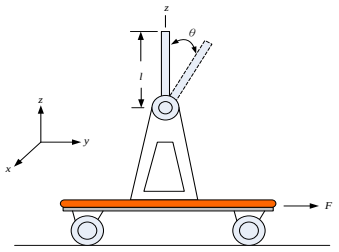

Figure 1. An inverted pendulum cart.

In the Fig. 1, the image processing methods used to get the cart positions and rod angles of the inverted pendulum is adaptive, in which images servo controller not only maintain the rod in up sate but also locate cart in the setting positions. A dc brush motor is used for the inverted pendulum. The model

Ying-Shing Shiao, Keng-Hao Chang, Ching-Wei Wu, Yun-Hao Tsai
National Changhua University of Education
Taiwan
justin927927@gmail.com

of a dc brush motor is shown in Fig. 2. The relationships of terminal voltage, speed, and torque are shown in (1)

$$T = K_1 i_a, \quad V_{emf} = k_2 \omega, \quad \text{and} \quad e - V_{emf} = R_a i_a, \tag{1}$$

where is torque, is torque constant (Nm/A), is armature current, is the back-EMF, is speed constant (V/rad/sec), is speed, is motor terminal voltage, and is armature resistance. The motor is applied voltage to generate armature and output torque. In case of not consider the frictional force, the motor torque applied a force on the wheels is:

$$F = \frac{T}{r} \tag{2}$$

where is the radius of wheels. By the relationships of (1) and (2) get the thrust of an inverted pendulum cart as the following:

$$F = \frac{K_1 e - K_1 K_2 \omega}{R_a r} \tag{3}$$

The wheel speed w and horizontal moving speed $\dot{y}(t)$ can be represented by the following:

$$\omega = \frac{\dot{y}}{r} \tag{4}$$

The kinetic energy is related with cart moving and rod rotation. The linear equations of the inverted pendulum are:

$$F = (M+m)\ddot{y} + ml\ddot{\theta} \tag{5}$$

$$m\ddot{y} + m\ell\ddot{\theta} - mg\theta = 0 \tag{6}$$

$$\ddot{\theta} = \frac{g}{\ell}\theta - \frac{\ddot{y}}{\ell} \tag{7}$$

where M is cart mass, m is rod mass, ℓ is rod length, $\ddot{y}$ is cart acceleration, θ is rod angle, $\ddot{\theta}$ is angular velocity, $g = 9.8 m/\sec^2$. Equation (3) is substituted into (5) and (6) is substituted into (8) to obtain:

$$\ddot{y} + \frac{k_1 k_2}{MR_a r^2}\dot{y} + \frac{mg}{M}\theta = \frac{k_1}{MR_a r} e \tag{8}$$

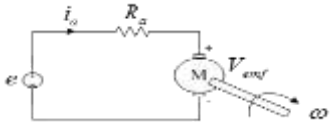

Figure 2. Equivalent circuit of DC motor.

Equation (8) is substituted into (7), the following equation is obtained.

$$\ddot{\theta} - \frac{(M+m)g}{Ml}\theta - \frac{k_1 k_2}{MlR_a r^2}\dot{y} = -\frac{k_1}{MlR_a r} e \tag{9}$$

Equation (8) and (9) is the model of an inverted pendulum, which is cast in state space form:

$$\begin{aligned} \dot{x} &= Ax + Be \\ Z_1 &= Cx \end{aligned} \tag{10}$$

where

$$x = \begin{bmatrix} y \\ \theta \\ \dot{y} \\ \dot{\theta} \end{bmatrix} \quad A = \begin{bmatrix} 0 & 0 & 1 & 0 \\ 0 & 0 & 0 & 1 \\ 0 & -\frac{mg}{M} & -\frac{k_1 k_2}{MR_a r^2} & 0 \\ 0 & \frac{(M+m)g}{Ml} & \frac{k_1 k_2}{MlR_a r^2} & 0 \end{bmatrix}$$

$$B = \begin{bmatrix} 0 \\ 0 \\ \frac{k_1}{MlR_a r} \\ -\frac{k_1}{MlR_a r} \end{bmatrix} \quad C = \begin{bmatrix} 1 & 0 & 0 & 0 \\ 0 & 1 & 0 & 0 \end{bmatrix}$$

An inverted pendulum's parameters are shown in Table 1.

TABLE I. THE PARAMETERS OF AN INVERTED PENDULUM

Parameter	Name	Value
r	cart wheel radius	0.0465 m
M	cart mass	7.93 kg
m	rod mass	0.364 kg
ℓ	rod length	0.222 m
k_1	motor torque-current constant	$113.99*10^{-3}$ Nm/A
k_2	motor voltage-speed constant	$1.934*10^{-3}$ V/rad/sec
R_a	armature resistance	1.93 Ω

The parameters of Table 1 are substituted into (10), we obtain

$$\dot{x} = \begin{bmatrix} 0 & 0 & 1 & 0 \\ 0 & 0 & 0 & 1 \\ 0 & -0.45 & -0.0066 & 0 \\ 0 & 46.2 & 0.0296 & 0 \end{bmatrix} x + \begin{bmatrix} 0 \\ 0 \\ 0.16 \\ -0.72 \end{bmatrix} e \tag{11}$$

The DC motor drives the cart that is controlled as the follows:

$$e = -K\hat{x} \tag{12}$$

where is the controller gain and is the measured state space variables of the inverted pendulum. Due to pole placement of a fixed gain may not be appropriate. Controller gain obtained by LQR control law is adopted. For optimization, the minimized cost function is the follows:

$$J = \int_0^\infty [x^T(t) Q x(t) + e^T(t)\,\mathrm{Re}(t)]dt \tag{13}$$

where Q is semi-positive definite matrix and R is positive definite matrix. Matrix Q and matrix R are endowed with physical meaning. Q is set to a diagonal matrix and R is set to a unit matrix. $Q = diag(q_1, q_2, q_3, q_4)$ where q_1 , q_2 , q_3 and q_4 correspond to y , θ , $\dot{y}$ and $\dot{\theta}$, respectively. The matrix elements of Q are considered with the degree of importance, therefore $q_1 \gg q_3$ as well as $q_2 \gg q_4$ are chosen. It is convenient to set $Q = diag(1000,1000,1,1)$ and $R = 1$, which are substituted to Riccati Equation [12] as:

$$A^T P + PA - PBR^{-1}B^T P + Q = 0 \tag{14}$$

Using (14) obtains the matrix that can be represented as:

$$e = -R^{-1}B^T P\hat{x} = -k\hat{x} \tag{15}$$

By manipulation obtain the controller gain $K=[-31.62 \quad -206.6 \quad -30.35 \quad -30.3]$ and the closed loop eigenvalues are $-6.992\pm1.587j$ and $-1.492\pm1.457j$.

As (12) shown the controller need the state space variables. Rod angles and cart positions are obtained by image processing. Therefore, the other two state variables, rod angular velocity $\dot{\theta}$ and cart velocity $\dot{y}$ have to be determined. These velocity variables are obtained by reduced order method [13]. Both states are represented as $Z=[Z_1 \quad Z_2]^T$. Let $Z_2=Tx$ represent where T is any matrix. Matrix C and matrix T are combined as $E=[C \quad T]^T$ which inverse is represented as $E^{-1}=[P|M]$. Z_1 and Z_2 are manipulated as:

$$\begin{bmatrix}Z_1\\Z_2\end{bmatrix}=\begin{bmatrix}C\\T\end{bmatrix}x \quad \rightarrow \quad x=\begin{bmatrix}C\\T\end{bmatrix}^{-1}\begin{bmatrix}Z_1\\Z_2\end{bmatrix}=[P|M]\begin{bmatrix}Z_1\\Z_2\end{bmatrix}=PZ_1+MZ_2 \quad (16)$$

The dynamic model of (10) is rewritten as the follow:

$$E\dot{x}=EAx+EBe \quad (17)$$

where A_{11}, A_{12}, A_{21} and A_{22} are 2×2 matrix and B_1 and B_2 are 2×1 matrix. They are sub matrix of A and B shown in (10). The observer for Z_2 is designed by the following approaches. Replace Z_2 by $\hat{Z}_2$, and add an error term for (17) after rearranging that is

$$\dot{\hat{Z}}_2=A_{21}Z_1+A_{22}\hat{Z}_2+B_2e+L(Z_1-C\hat{x}) \quad (18)$$

Let $w\cong\hat{Z}_2-LZ_1$, after manipulation the reduced-order observer can be obtained:

$$\begin{aligned}\dot{w}&=Fw+DZ_1+Gu\\ \hat{x}&=Mw+NZ_1\end{aligned} \quad (19)$$

where $F\cong A_{22}-LA_{12}$, $D\cong FL+A_{21}-LA_{11}$, $G\cong B_2-LB_1$, $N\cong P+ML$. The math tool, Matlab, is used to find the matrix as:

$$>>\text{L=lqr}(A_{22}', A_{12}', Q_O, R_O) \quad (20)$$

where matrix Q_o and matrix R_o are used for adjustment, after different weight test $Q_O=diag(1,500)$ and $R_O=1$ are adopted for (20) to obtain $L=\begin{bmatrix}0.9934 & 0.0013\\ 0.0013 & 22.3607\end{bmatrix}$. The matrix L is substituted into (19) to obtain:

$$\dot{\omega}=\begin{pmatrix}-1.0 & -0.0013\\ 0.0283 & -22.36\end{pmatrix}\omega+\begin{pmatrix}-0.993 & -0.479\\ 0.0 & -453.8\end{pmatrix}Z_1+\begin{pmatrix}0.16\\ -0.72\end{pmatrix}e \quad (21)$$

$$\hat{x}=\begin{pmatrix}1 & 0\\ 0 & 1\\ 0.993 & 0.0013\\ 0.0013 & 22.360\end{pmatrix}Z_1+\begin{pmatrix}0 & 0\\ 0 & 0\\ 1 & 0\\ 0 & 1\end{pmatrix}\omega \quad (22)$$

Finally, the and back to Eq. (12) give

$$e=61.81y+884.2\theta+30.35w_1+30.3w_2 \quad (23)$$

where w_1 is the observed cart velocity and w_2 is the observed rod angular velocity.

III. Image-based Controller

Image enhancement highlights the features of an image so as to obtain the rod and cart segment used to determine the rod angles and cart positions. The gray level of an image is $I_o(x,y)$, the gray level adjustment is shown as:

$$I_N(x,y)=I_O(x,y)+K_1 \quad (24)$$

where $I_N(x,y)$ is the image after adjustment, K_1 is a adjustment constant which range is -128 to 127. Resolutions of an inverted pendulum image are effect upon illumination, dynamic range of a CCD, lens aperture, etc. Poor contrast of an images caused by these effects cannot be treated well by (24). Image enhancement is the way for improving poor image contrast. The image intensity adjustment is shown as:

$$I_P(x,y)=(I_O(x,y)-128)\tan k_2+128 \quad (25)$$

where I_P is the enhancement image, K_2 is the adjustment parameters which range is 1 to 89. Using (24) and (25) to adjust brightness and contrast of Fig. 3 (a) and selecting an appropriate threshold get a clear binary image shown in Fig. 3 (b).

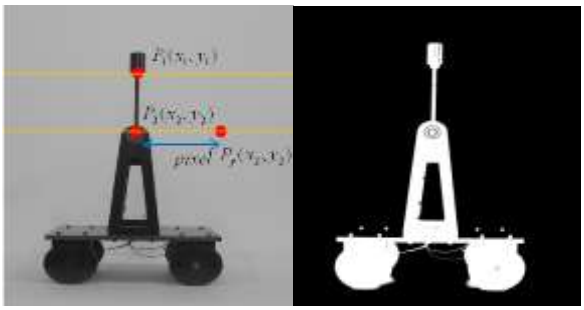

(a) (b)

Figure 3. (a) An inverted pendulum cart. (b) The binary image of an inverted pendulum.

The pendulum center and the rod are obviously shown in the binary image. It is convenient to separate the rod and cart from this binary image. As shown in Fig. 3 (a), pixels $P_1(x,y)$ and $P_2(x,y)$ on the boundary of rod image are used to determine the rod angle. Pixel $P_2(x,y)$ is used as the cart position in case of the rod is vertically up.

In the binary image of an inverted pendulum, two fixed horizontal lines are chosen for searching two pixels $P_1(x_1,y_1)$ and $P_2(x_2,y_2)$ of the rod boundary shown in Fig. 3 (a). On the chosen lines, searching from left to right where the pixels are logical one and its right neighbor is logical zero. They are the candidate points of the rod boundary. Using P_1 and P_2, we can find the rod angle θ shown as the follow:

$$\sin\theta=\frac{x_1-x_2}{\sqrt{(x_2-x_1)^2+(y_2-y_1)^2}} \quad (26)$$

Assumed the motion of the rod without change drastically, it is convenient to let $\sin\theta\cong\theta$. Because y_2-y_1 is a constant, the rod angle is determined by using the follow:

$$\theta = \frac{x_2 - x_1}{\sqrt{(x_2 - x_1)^2 + C^2}} \tag{27}$$

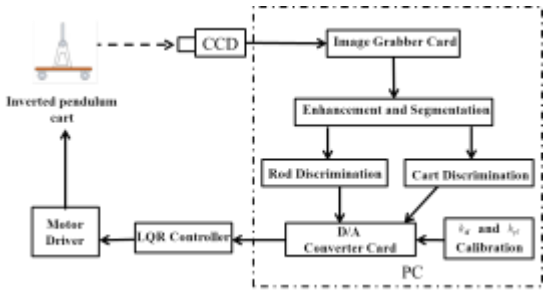

Figure 4. An inverted pendulum system with an image-based controller.

The signals of rod angles and cart positions are measured by image procession and used for the LQR controller to form an image-based controller. As shown in Fig. 4, the rod angles and cart positions are measuring by a CCD camera, image processing, and D/A converter. The measured results are output to the LQR controller's input. The D/A converter output levels and the LQR controller input level must to avoid be inconsistent making the inverted pendulum not in controllable. In image processing the measured cart positions and rod angles is pixels which output by D/A converter is volt. The measured cart position gain K_{yI} and rod angle gain $K_{\theta I}$ must be calibrated, respectively. The rod angle measured by (27) and its output by D/A converter is voltage V_θ that can be expressed as the follow:

$$V_\theta = \frac{V_{\theta \max}}{180^0} \times \theta = K_{\theta I} \times \theta \tag{28}$$

where $V_{\theta \max}$ is the maximum output voltage of the D/A converter. By (28) the rod angle gain $K_{\theta I}$ is obtained. As shown in Fig. 3(a), the initial cart position is set at $P_2(x_2, y_2)$ and the measured cart position is $P_y(x_2, y_2)$, respectively, as the follow:

$$V_{oy} = (P_y(x_2, y_2) - P_2(x_2, y_2)) \times K_{yI} \tag{29}$$

where V_{oy} is the measured cart position in volt and K_{yI} is the cart position gain. The maximum of cart moving in the grabbed image is $K_{yp}\ pixel$, and the maximum output voltage of the D/A card is $V_{yI\max}$ that obtain the cart position gain K_{yI} is $V_{y\max}/K_{yp}$.

IV. Experimental Results

The experimental results are shown in Fig. 5. Fig. 5 (a) is the initial state of an invented pendulum, in which the rod is at upright and the cart is at the reference position. Fig. 5(b) is the scheme of the cart is not at the reference position. The experimental result shows the inverted pendulum slowly move to the reference position and shows the rod remain immobility during cart moving. The experimental result of a hit on the rod is shown in Fig. 5(c) in which the responses of the cart moving and the rod swing shows the image-based controller controls the cart motion to maintain the rod in the upright state. Although the proposed image-based controller controls an inverter pendulum to swing back and forth 5-6 times before stabilized, its response may slower than the conventional methods using potentiometers to measure the rod angles and the cart positions. If the methods of proposed image processing are implemented by the hardware, the image-based controller will get a better response. The consecutive images of a moving inverted pendulum cart are shown in Fig. 6.

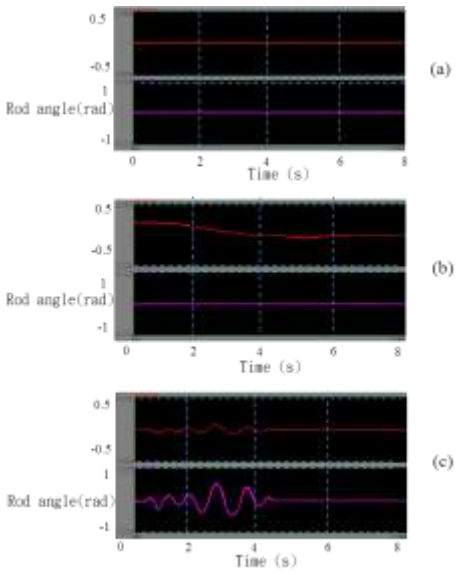

Figure 5. The experimental results of (a) the cart and the rod are in balance, (b) the cart back to its origin, and (c) the rod with a hit.

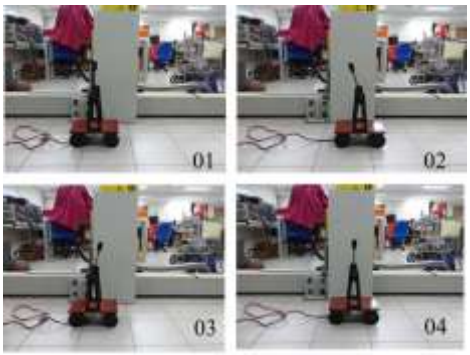

Figure 6. A moving inverted pendulum cart.

V. Conclusion

This paper proposes an image-based controller which uses a camera and image processing methods to measure the rod angles and cart positions for an inverted pendulum. This method illustrated speed limit such as on sale camera can be a non-contact measuring device used for controller. The illumination is a key factor which affects the results of image processing. The enhancement algorithms are designed to segment the rod and cart image that obtain the measurement reliability of rod angle gain and cart position gain. The

experimental results demonstrate that the proposed image-based controller with the performances as the conventional methods. After an external force to interfere the rod, the proposed image-based controller can control an inverted pendulum back to the equilibrium point. Non-contact measurement is an advantage of visual servo control that facilitate an inverted pendulum with the ability moving to an arbitrarily position. But, the lighting has to be propriety setting and the response is limit.

References

[1] A. S. Shiriaev, A. Friesel, J. Perram, and A. Pogromsky, "On Stabilization of Rotational Modes of an Inverted Pendulum," Proceedings of the 39th IEEE Conference, Decision and Control, Vol. 5, pp. 5047–5052, 2000.

[2] A. Inoue, M. Deng, and T. Tanabe, "Practical Swing-up Control System Design of Cart-type Double Inverted Pendulum," Proceedings of the 25th Chinese Control Conference, pp. 2141-2146, 2006.

[3] K. G. Eltohamy and C.Y. Kuo, "Real Time Stabilisation of a Triple Link Inverted Pendulum Using Single Control Input," IEE Proceedings Control Theory and Applications, Vol. l44, No. 5, pp. 498-504, 1997.

[4] Z. Yu, S. Luo, Z. Lv, and L. Wu, "Control Parallel Double Inverted Pendulum by Hierarchical Reinforcement Learning," Proceedings of the 7th ICSP International Conference on Signal Processing, Vol. 2, pp. 1614-1617, 2004.

[5] S. Nundrakwang, T. Benjanarasuth, J. Ngamwiwit, and N. Komine, "Hybrid Controller for Swinging up Inverted Pendulum System," Information, Communications and Signal Processing, 2005 Fifth International Conference on 06-09, pp. 488-492, 2005.

[6] H. Hiroshi, H. Koji, A. Masatoshi, O. Shigeto, and A. Masatoshi, "Self-Tuning Control for Rotation Type Inverted Pendulum Using Two Kinds of Adaptive Controllers," IEEE International Conference on Automation and Logistics, pp.1-6, 2006.

[7] M. E. Magana, and F. Holzapfel, "Fuzzy-Logic Control of an Inverted Pendulum with Vision Feedback," IEEE Transactions on Education, Vol. 4, No. 1, pp. 165-170, 1998.

[8] B. Kosko, Neural Networks and Fuzzy Systems. Englewood Cliffs, NJ:Prentice-Hall, 1992.

[9] L. Wang, Adaptive Fuzzy Systems and Control: Design and Stability Analysis, Englewood Cliffs, NJ: Prentice-Hall, 1994.

[10] T. Brem and T. Rattan, "Hybrid Fuzzy Logic PID Controller," Proceedings of the IEEE 1993 National Aerospace and Electronics Conference, pp. 807–813, 1993.

[11] M. I. H. Nour, J. Ooi, and K. Y. Chan, "Fuzzy Logic Control vs. Conventional PID Control of an Inverted Pendulum Robot," International Conference on Intelligent and Advanced Systems , pp. 209 – 214, 2007.

[12] X. Chen, H. Zhou, R. Ma, F. Zuo, G. Zhai, and M. Gong, "Linear Motor Driven Inverted Pendulum and LQR Controller Design," IEEE International Conference on Automation and Logistics, pp.1750-1754, 2007.

[13] Dongil Choi and Jun-ho Oh, "Human-friendly motion control of a wheeled inverted pendulum by reduced-order disturbance observer," IEEE International Conference on Robotics and Automation, pp. 2521-2526, 2008.

About Author (s):

Ying-Shing Shiao received the Ph.D. in Electrical Engineering from National Cheng Kung University in 1992. He is a Professor in Department of Electrical Engineering, National Changhua University of Education, Changhua, Taiwan. His research interest includes computer vision, digital image processing, control engineering, and intelligent robot.

Keng-Hao Chang received the B.S. degree in Electrical Engineering from National Changhua University of Education in 2012. He is pursuing the M.S. degree in Department of Electrical Engineering, National Changhua University of Education, Changhua, Taiwan. His current research interests include quadrotor, visual control and computer vision.

Ching-Wei Wu received the M.S. in Electrical Engineering from National Changhua University of Education in 2009. He is pursuing the Ph.D. degree in Department of Electrical Engineering, National Changhua University of Education, Changhua, Taiwan. His current research interests include visual control and computer vision.

Yun-Hao Tsai received the B.S. degree in Electrical Engineering from Southern Taiwan University of Science and Technology in 2011. He is pursuing the M.S. degree in Department of Electrical Engineering, National Changhua University of Education, Changhua, Taiwan. His current research interests include visual control and computer vision.